NRL Memorandum Report 4472

Convective Cooling of Lightning Channels

J. M. Picone and J. P. Boris

Laboratory for Computational Physics

J. R. Greig and M. Raleigh

Experimental Plasma Physics Branch
Plasma Physics Division

and

R. F. Fernsler

JAYCOR, Inc.
Alexandria, VA 22304

April 14, 1981

This research was supported by the Office of Naval Research and by the Defense Advanced Research Projects Agency (DoD) ARPA Order No. 3718, monitored by the Naval Surface Weapons Center under Contract N60921-80-WR-W0189.

NAVAL RESEARCH LABORATORY
Washington, D.C.

(14) NRL-MR-4472

SECURITY CLASSIFICATION OF THIS PAGE (When Data Entered)

(9) REPORT DOCUMENTATION PAGE

READ INSTRUCTIONS BEFORE COMPLETING FORM

1. REPORT NUMBER: NRL Memorandum Report 4472

2. GOVT ACCESSION NO.: AD-A097994

3. RECIPIENT'S CATALOG NUMBER:

4. TITLE (and Subtitle): (6) CONVECTIVE COOLING OF LIGHTNING CHANNELS.

5. TYPE OF REPORT & PERIOD COVERED: Interim report on a continuing NRL problem.

6. PERFORMING ORG. REPORT NUMBER: (15) ARPA Order-3718

7. AUTHOR(s): (10) J. M. Picone, J. P. Boris, J. R. Greig, M. Raleigh and R. F. Fernsler*

8. CONTRACT OR GRANT NUMBER(s):

9. PERFORMING ORGANIZATION NAME AND ADDRESS:
Naval Research Laboratory
Washington, DC 20375

(12) 29

10. PROGRAM ELEMENT, PROJECT, TASK AREA & WORK UNIT NUMBERS: (17)
61153N; RRØ330244; 44-0756-0-1
and 61101E; 0; OR40AA

11. CONTROLLING OFFICE NAME AND ADDRESS:
Office of Naval Research, Arlington, VA 22217 and
Defense Advanced Research Projects Agency,
Arlington, VA 22209

(11) 14

12. REPORT DATE: Apr[redacted]981

13. NUMBER OF PAGES: 28

14. MONITORING AGENCY NAME & ADDRESS (if different from Controlling Office):
Naval Surface Weapons Center
White Oak, MD 20910

(16) RRØ33Ø2

15. SECURITY CLASS. (of this report): UNCLASSIFIED

15a. DECLASSIFICATION/DOWNGRADING SCHEDULE:

16. DISTRIBUTION STATEMENT (of this Report):

Approved for public release; distribution unlimited.

17. DISTRIBUTION STATEMENT (of the abstract entered in Block 20, if different from Report):

18. SUPPLEMENTARY NOTES:

This research was supported by the Office of Naval Research and by the Defense Advanced Research Projects Agency (DoD) ARPA Order No. 3718, monitored by the Naval Surface Weapons Center under Contract N60921-80-WR-W0189.

*Present address: JAYCOR, Inc., Alexandria, VA 22304

19. KEY WORDS (Continue on reverse side if necessary and identify by block number):

Lightning
Nitrogen fixation
Convective cooling
Electric discharges

20. ABSTRACT (Continue on reverse side if necessary and identify by block number):

We report experimental data which trace the time development of electric discharge channels in air and which demonstrate the turbulent cooling of such channels. These data provide qualitative confirmation of the model proposed and used by Hill, Rinker, and Wilson to calculate the production of nitrogen oxides by lightning. We outline an analytical treatment which identifies assymmetries in the pressure and density gradients of the discharge channel as a significant source of vorticity. The vorticity, in turn, causes ambient air to mix into the channel. Our theoretical analysis results in

(Continues)

DD FORM 1 JAN 73 1473 EDITION OF 1 NOV 65 IS OBSOLETE
S/N 0102-014-6601

SECURITY CLASSIFICATION OF THIS PAGE (When Data Entered)

251950

20. ABSTRACT (Continued)

equations from which the vorticity strength and mixing time scale may be calculated. We briefly describe detailed simulations with which we have calibrated the theory. Finally, we combine the experimental data with our calibrated formulas to estimate the convective mixing rate in the case of lightning. We obtain a rate of $\sim 300\ cm^3$/sec per cm^3 air in the return stroke channel after pressure equilibrium has been achieved.

about 300 cc/sec/cc

CONTENTS

CONVECTIVE COOLING OF LIGHTNING CHANNELS

1. Introduction

Hill et al. (1980) have recently proposed a "channel heating" model to predict the production of atmospheric nitrogen oxides (NO_x) by lightning. In this model, the return stroke deposits energy over ~100μs, heating the lightning channel to ~30000K within a few microseconds. As energy is deposited, the heated region (i.e., the channel) expands and compresses the atmosphere surrounding the channel to produce a shock wave. Subsequently, the shock wave decouples from the channel as the return stroke current drops to small values. The channel continues to expand until pressure equilibrium is reached with the surrounding air at a temperature of ~3000K. The rate at which the air inside the channel cools is important to the calculation of NO_x production by lightning. Hill et al. (1980) calculated the production rate based on the assumption of "turbulent" or convective cooling, in which the ambient air is mixed with the air inside the channel at a prescribed constant rate. The authors used a detailed air chemistry computer code to simulate cooling at several rates, the lower limit of which was based on the rate of cooling by thermal conduction in the absence of convective mixing. They left open questions regarding the cause of the convective cooling, the efficiency of mixing, and the length of the time interval between pressure equilibration of the channel and the onset of mixing.

In this note, we report experimental data which directly confirm qualitative aspects of the above model and which demonstrate the turbulent cooling of discharge channels. We then outline a preliminary analytical treatment which identifies asymmetries in the pressure and density gradients of the discharge channel as a significant source of vorticity, which in turn causes the ambient air to mix into the channel. Our theoretical analysis results

Manuscript submitted January 12, 1981.

in equations from which the vorticity strength and the mixing time scale may be calculated. To calibrate this analytic model and test its predictions, we have performed detailed, two-dimensional numerical simulations which will be described briefly and compared with our analytic results. Finally, we combine the experimental data with our calibrated formulas to estimate the convective mixing rate in the case of lightning.

2. Experimental Studies

We have recently performed experimental studies of the propagation of electric discharges through air and the dynamics of the resulting channels (Greig, et al., 1978). In Fig. 1, we show Schlieren photographs of discharges which were 15 cm in length. The discharges were produced by a Marx generator with an erected voltage of ~250 kV. The current had a peak value of ~10 kA, a period of ~3μs, and a duration of ~6μs. While this is a much shorter pulse than that occurring in a lightning return stroke, we expect the qualitative behavior to be similar after the shock decouples from the channel because air response in rotational flow is relatively slow. We have, in fact, performed preliminary experiments using parameters similar to those of a lightning return stroke. We could not, however, obtain a complete sequence of photographs similar to Fig. 1 because the channel size exceeded the capability of our optical system.

In Fig. 1, we see that a hot, smooth, curved channel with a radius of ~1.4 cm has formed within 8μs of the initiation of the discharge. The accompanying shock wave has already decoupled from the channel and appears as a sharp line at the boundary. By 30μs, the shock is easily identifiable and propagates out of the field of view at a time somewhat greater than 100μs after discharge initiation. At approximately 100μs, the interior temperature of the channel is ~5000K, the gas density is $\sim 10^{18}\,cm^{-3}$ and the electron density is

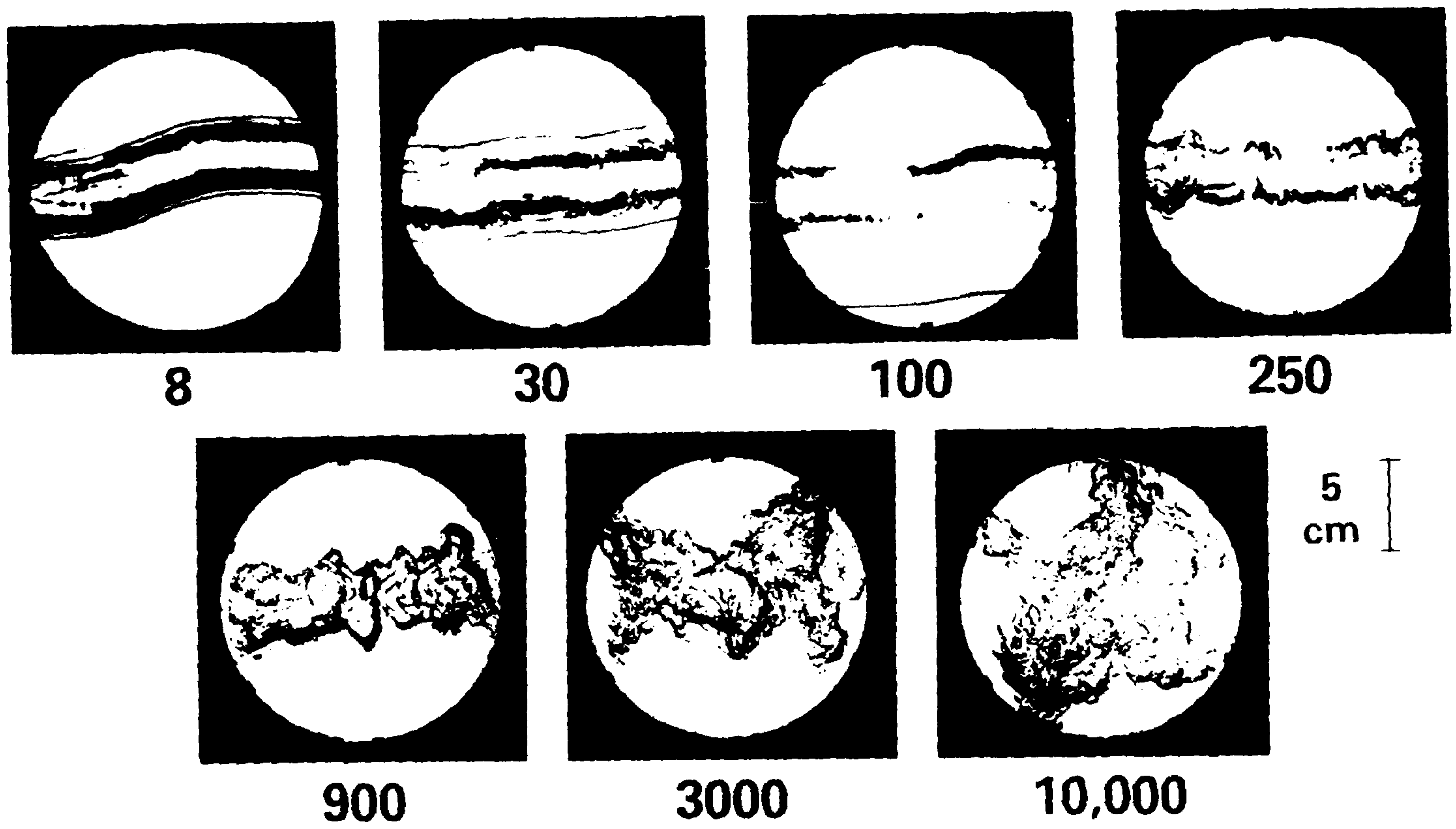

Fig. 1 – *Schlieren photographs of unguided discharges in the atmosphere; discharge length 15 cm; voltage ~ 250 kV. The time at which each photograph was taken is given in microseconds; the exposure time was 25 nsec. Note that the photographs depict separate, nominally identical discharges.*

$\sim 10^{14} cm^{-3}$. (These values are the measured conditions for a comparable discharge in a pre-ionized channel.) The heated channel remains roughly stable up to that point. By 250μs, however, instability has begun to distort the channel, as evidenced by density fluctuations at the channel boundary. The photograph at 900μs shows that the distortions become more pronounced as cooler air at the edges of the channel is pulled toward the axis. The average radius has also increased to $\sim$ 2cm, indicating an increase of $\sim$ 100% in the volume of the channel due to entrainment of the surrounding air. As the time from discharge initiation increases, smaller scale (turbulent) structure appears and by 10ms, the channel has begun to disappear. We estimate the final channel radius to be $\sim$ 6-7cm, indicating a volume increase of $\sim$ 20 times the original volume. Studies of similar discharges, which have been guided along a path designated by laser/aerosol interaction, have produced nearly identical results. Channel cooling and the onset of turbulence were somewhat more rapid for such "laser-guided discharges." This result follows directly from the analytic theory described in the next section.

3. Theoretical and numerical studies

Our theoretical treatment[2] attributes the "turbulent" (convective) cooling phenomenon to asymmetries between the gradients of the existing pressure and density distributions. These asymmetries will generate vorticity as the channel expands, according to the equation

$$\frac{d\underset{\sim}{\xi}}{dt} + \underset{\sim}{\xi}\,\underset{\sim}{\nabla} \cdot \underset{\sim}{v} = \underset{\sim}{\xi} \cdot \underset{\sim}{\nabla}\,\underset{\sim}{v} + (\underset{\sim}{\nabla}\rho \times \underset{\sim}{\nabla}P)/\rho^2, \tag{1}$$

where

$$\underset{\sim}{\xi} = \underset{\sim}{\nabla} \times \underset{\sim}{v} \tag{2}$$

is the vorticity, $\underset{\sim}{v}$ is the fluid velocity, ρ is the density, and P is the pressure. All of the variables are functions of the position $\underset{\sim}{r}$ and the time t. Following expansion of the channel to achieve pressure equilibrium,

a significant residual vorticity exists. This vorticity is responsible for mixing of ambient air with the hot channel gas. We should point out that other mechanisms for generating residual vorticity in the heated channel might exist. For example, rapid movement of the discharge current axis may occur as a result of magnetic forces present when the current is nonnegligible. Such movement could cause sufficient displacement of the surrounding air to produce some long-term mixing motion. We will reserve consideration of such phenomena for a future, more detailed paper.

We have identified several types of asymmetry which might be relevant to lightning and the above discharge experiments:

(1) Two-dimensional distortions of the return stroke channel from a circular cross section,

(2) Two-dimensional asymmetries from return stroke displacement off the axis of the leader stroke, and

(3) Three-dimensional distortions in the return stroke, such as the curvature of the channel axis shown in Fig. 1.

If we define a cylindrical coordinate system with the z-axis along the average direction of the channel axis (for channel sections which do not undergo large changes in direction), we find that all three types of asymmetry will produce a nonzero value of ξ_z. This will cause mixing in the (r,θ) plane. In addition, for three-dimensional asymmetries, ξ_θ will be non-negligible, producing mixing in the (r,z) plane (a vortex sheet). Fig. 2 shows that, for sufficiently short channel sections, all three types of asymmetry may be represented by a displacement $\underset{\sim}{X}_0$ in the (r,θ) plane, which causes the rotational symmetry about the z-axis to be broken. In our derivations, we will define the x-axis to be parallel to

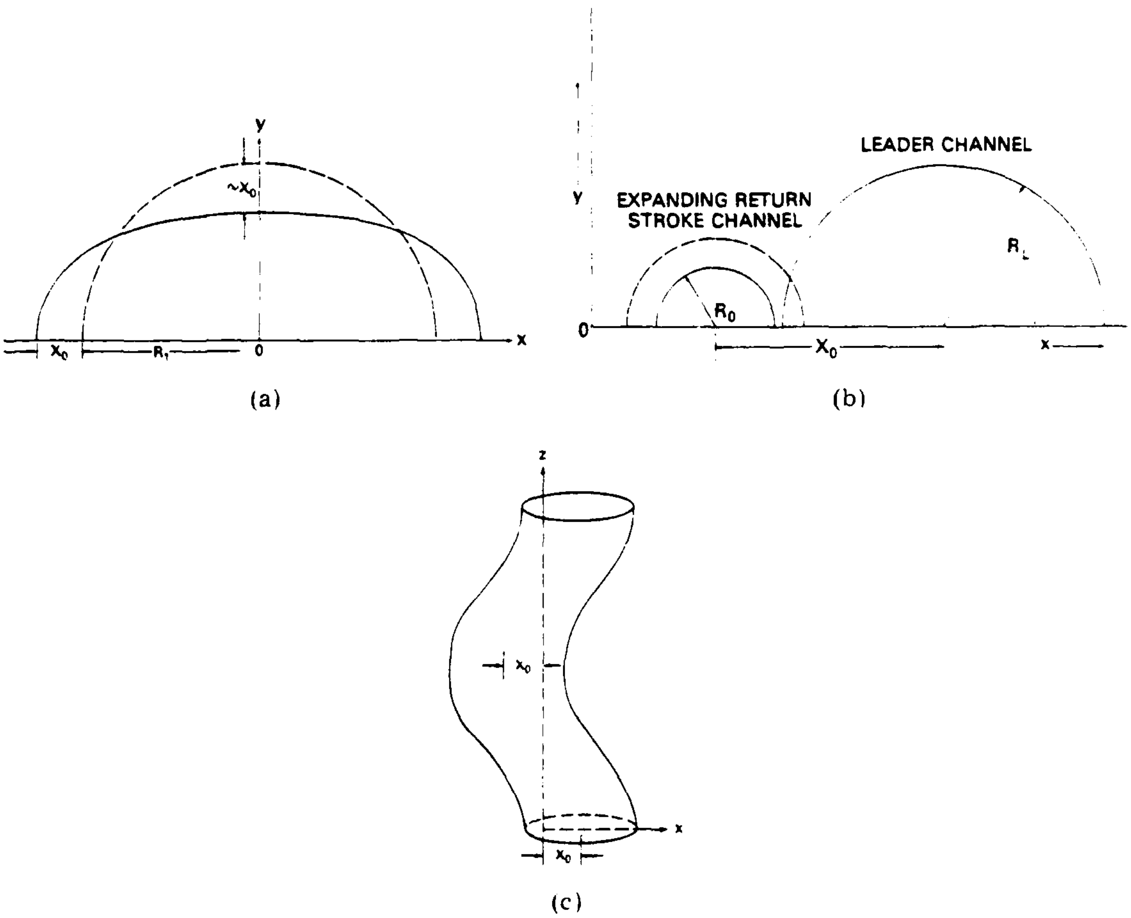

Fig. 2 — Schematic diagrams of three types of return stroke asymmetry which generate vorticity: (a) two-dimensional distortions (e.g., elliptical channel), (b) displacement from axis of leader channel, (c) three-dimensional distortions. The degree of asymmetry may be expressed in terms of the quantity X_0 as indicated. In Fig. 2a and 2b, we show only the portion above the $x - z$ symmetry plane.

$\underset{\sim}{X}_0$. With this convention, Fig. 3 shows the flow field in the x-y plane for cases b and c in Fig. 2 after the return stroke channel has reached pressure equilibrium with the ambient air. This flow pattern is approximately equivalent to that of a vortex filament pair having average strengths of $\pm\bar{\kappa}_z$ and located respectively at $(\bar{x}, \pm\bar{y})$. (The flow pattern for the elliptical channel in Fig. 2b is equivalent to the superposition of two vortex filament pairs. For simplicity we will discuss only a single vortex filament pair.) The average strength $\bar{\kappa}_z$ is given by (Batchelor, 1967)

$$\bar{\kappa}_z(\tau) = \int_0^\infty dy \int_{-\infty}^\infty dx \quad \xi_z(x,y,\tau) \tag{3}$$

and the coordinates are

$$\bar{x}(\tau) = \frac{1}{\bar{\kappa}_z(\tau)} \int_0^\infty dy \int_{-\infty}^\infty dx \quad x \quad \xi_z(x,y,\tau) \tag{4}$$

and

$$\bar{y}(\tau) = \frac{1}{\bar{\kappa}_z(\tau)} \int_0^\infty dy \int_{-\infty}^\infty dx \; y \; \xi_z(x,y,\tau) \tag{5}$$

We obtain $\xi_z(x,y,\tau)$ by integrating (1) over the time interval $(0,\tau)$, where $t = 0$ is the time of discharge initiation.

The vortex filament pair will migrate as a unit at a speed of

$$v_{pair} = \bar{\kappa}_z/4\pi\bar{y} \tag{6}$$

in a direction parallel to the x-axis. The fluid velocity along the x-axis is

$$v_x(x,0) = \bar{\kappa}_z \; \bar{y}/\pi(x^2 + \bar{y}^2) \tag{7}$$

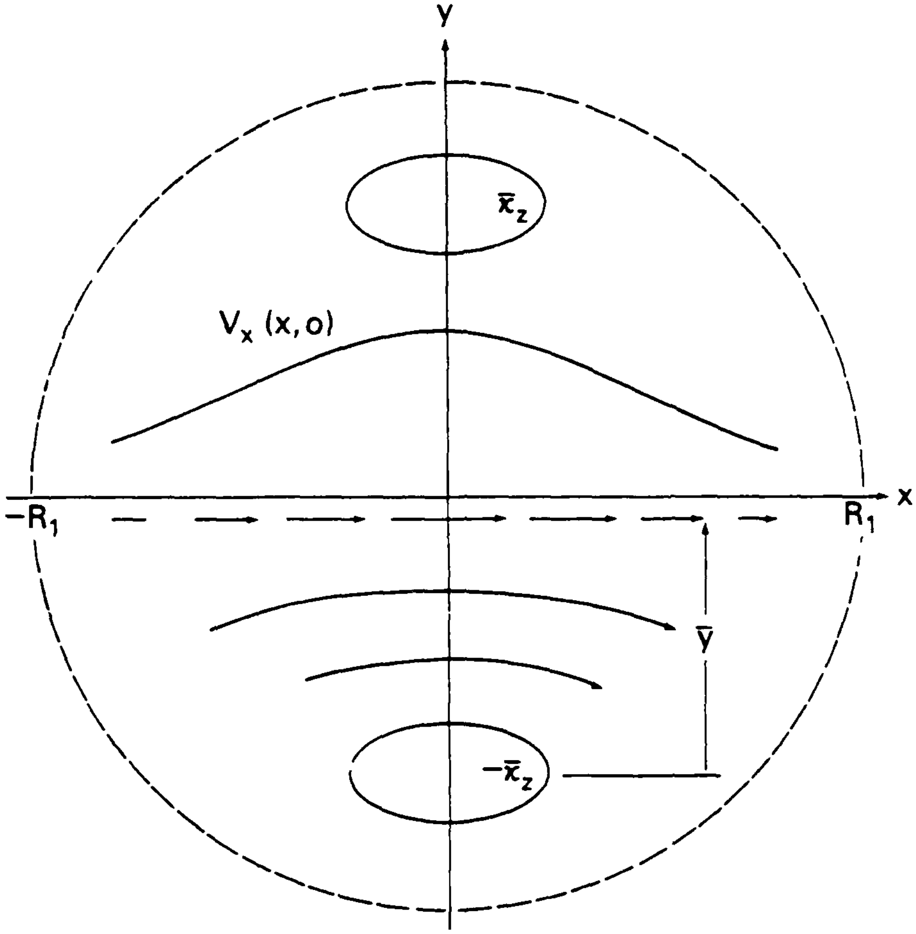

$$\tau_{mix} = \frac{2\pi R_1}{|\bar{\kappa}_z|\bar{y}} \left[R_1^2/3 + \bar{y}^2\right]$$

Fig. 3 — Symmetric distribution of localized vorticity appears as two extended vortex filaments $\bar{\kappa}_z$ separated by a distance $2\bar{y}$. Flow velocity induced by these vortices is shown along the x axis halfway between the filaments. The mixing time τ_{mix} is defined here as the time it takes a fluid element at $-R_1$ to reach R_1 and hence effectively bisect the hot channel.

If we define a characteristic mixing time scale τ_{mix} to be the time interval over which a fluid element travels along the x-axis from one "edge" of the channel to the opposite "edge," we may use (7) to obtain

$$\tau_{mix} = 2\pi R_1 (R_1^2/3 + \bar{y}^2)/|\bar{\kappa}_z|\bar{y} \tag{8}$$

where R_1 is the approximate radius of the return stroke channel when pressure equilibrium is reached. We may, therefore, characterize the mixing time scale if we know the vorticity strength and the average displacements of the equivalent vortex pair from the (x,z) symmetry plane.

We have performed the integral in (3) by using (1) in conjunction with the following assumptions:

(1) We treat the return stroke as an instantaneous pressure pulse of finite size with a given radial profile and with a total energy deposition equivalent to that of a return stroke. The assumption of instantaneous deposition fits closely the experimental situation of Fig. 1. At the same time, we do not parallel the work of Hill, (1971, 1979), who permits energy to be deposited over a time interval $\sim 100 \mu s$. However, the formalism which we have developed is adequate for this latter case as well.

(2) The time τ in (3) is equal to the time required for the return stroke channel to achieve pressure equilibrium with the surrounding atmosphere. For times $t > \tau$ a residual vorticity exists, and this vorticity is responsible for convective cooling of the lightning channel.

(3) During expansion of the return stroke channel, the fluid outside the expanding region behaves incompressibly and the interior region expands uniformly. Thus the radial dependence of the fluid velocity is given by

$$v_r(r, t) = \begin{cases} \dfrac{U(t)\, r}{R(t)} & r \le R(t) \\[2ex] \dfrac{U(t)\, R(t)}{r} & r > R(t) \end{cases} \tag{9}$$

where the boundary of the heated region is $R(t)$ and the velocity of the boundary is $U(t) = \dot{R}(t)$. This assumption appears to be reasonable since the shock wave carries away only about 10% of the total energy deposited by the return stroke. Further, this assumption is more accurate when the energy deposition is slower. Notice that the acceleration is radial and has values strictly appropriate only if the effects of the nonaligned density gradients on the driving expansion flow are small.

(4) We approximate the integrand in (3) in terms of its value at time $t=t_m$, at which the expansion flux $R_m U_m \equiv R(t_m)\, U(t_m)$ is a maximum. Under the above conditions, we obtain for the residual vorticity

$$\bar{\kappa}_z(t) \approx \bar{\kappa}_z(\tau) \approx U_m (R_1 - R_0)\, \ell n\, (\rho_\infty/\rho_0)\, f\, (R_0, R_1, R_m, X_0) \tag{10}$$

for the average z-component of the vorticity strength where $t \gtrsim \tau$. The quantities R_0 and R_1 are, respectively, the initial average radius of the heated (return stroke) region and the average radius following expansion, and ρ_∞ is the ambient density. The quantity ρ_0 is the density at the center of the return stroke channel for asymmetry types 1 and 3 (two and three dimensional distortions of the return stroke channel). For asymmetry type 2 (return stroke displacement off the leader channel axis), ρ_0 is the density at the center

of the leader channel. The dimensionless form factor f is a complicated integral which contains geometric effects, detailed hydrodynamical interactions and information about the leader and return stroke pressure and density profiles. For asymmetry type 2, we have evaluated the form factor, f_2, for several different pressure and density profiles and have found that f_2 is not strongly profile dependent. The values of $|f_2|$ vary smoothly from zero at $X_0/R_1 = 0$ to a peak of $\leqslant 0.5$ at $X_0/R_1 \sim 1$. The values then decrease somewhat more slowly to zero as X_0/R_1 increases beyond a value of ~ 1. Similar behavior occurs for the other asymmetry types. For rough estimates of $|\omega_z|$ a value of $|f| \sim \frac{1}{3}$ is permissible, and we may substitute c_s for U_m, where c_s is the speed of sound at the axis of the return stroke when the current flow begins ($t = 0$).

We have performed preliminary detailed simulations of the problem using the FAST2D computer code (Boris, 1977) to validate and calibrate the approximate analytic model developed above. In addition to accounting for shocks properly, which the theoretical model does not do, the simulations are capable of describing the late-time motions and profiles as modified by the induced vorticity. As above, we have treated the return stroke as an instantaneous pulse of finite size and equivalent energy rather than depositing the energy over a characteristic time interval ($\sim$100 μs). These simulations have indicated that the above analytic model and the resulting formula given in (10) will, in most cases, provide estimates of $\bar{\omega}_z$ which differ from the simulation results by less than 30%. We have discovered that only modest asymmetry ($X_0 \sim R_1/10$) is required to generate considerable mixing and that for a wide range of values of X_0/R_1 ($0.1 \lesssim X_0/R_1 \lesssim 1.5$) the residual vorticity and mixing rate vary by less than 30%.

Preliminary investigations of the asymmetries of type (3), i.e., three-dimensional distortions of the return stroke profile, indicate that (10) holds for $\bar{\lambda}_{\theta}$ as well. For cases in which more than one type of asymmetry are present, the cumulative effects should increase the mixing rate, and the channel should cool more quickly. This would explain the faster cooling rates for electric discharges guided by preformed laser channels, since some displacement of the discharge axis from the axis of the preformed laser channel would be expected as well as three-dimensional distortion of the electric discharge channel.

We can now analyze the mixing shown in Fig. 1, which we assume in this case to be due primarily to three-dimensional curvature with a value of $X_0/R_1 \sim 0.25$. We have $R_0 \sim 0.1$ cm (measured from open shutter photographs of the discharges), $R_1 \sim 1.4$ cm, $\rho_\infty/\rho_0 \sim 10$, $|f_3| \sim \frac{1}{3}$ and $U_m \sim c_s \sim 3.5 \times 10^4$ cm/s. From (10) we calculate $\bar{\lambda}_z \sim 3.5 \times 10^4$ cm^2/s. Using (8), and $\bar{y} \sim 0.8\ R_1$ (from our simulations), we obtain $\tau_{mix} \simeq 430$ μs. From Fig. 1, we notice that violent perturbations begin to occur sometime between $\sim 250\mu$s and $\sim 900\mu$s. This is consistent with the definition and value of τ_{mix}.

From Fig. 1, we also find that, for the laboratory experiments, reasonably complete mixing occurs at a time $\Delta t_{cool} \sim 10^4 \mu$s, which is $\sim 20\tau_{mix}$ following discharge initiation. Referring to our discussion of the laboratory discharges in Fig. 1, we see that the volume increase of the channel ΔV_{cool} (during the interval Δt_{cool}) is also $\sim 20\ V_0$, where V_0 is the initial volume. We have found that, in general for convective cooling, (Appendix A),

$$\frac{\Delta t_{cool}}{\tau_{mix}} \approx \frac{\Delta V_{cool}}{V_0} . \tag{11}$$

The ratio on the right hand side of (11) depends only on the temperature of the channel before appreciable mixing occurs and the ambient temperature. For our laboratory discharges and lightning, these temperatures are approximately

the same. Thus, we assume that for lightning $\Delta t_{cool} \sim 20\ \tau_{mix}$, from which we may obtain rough estimates of the time required for "complete" cooling of a return stroke channel and of the average mixing rate. For lightning we assume (Hill <u>et al</u>.,1980) $R_0 \sim 1$cm, $R_1 \sim 16$cm, $\rho_\infty/\rho_0 \sim 10$, $|f| \sim \frac{1}{3}$, and $U_m \sim c_s \sim 5\text{x}10^4$cm/s. From (10) we obtain $\bar{\kappa}_z \sim 58\text{x}10^4 \text{cm}^2/\text{s}$. Using (8) with $\bar{y} \sim 0.8\ R_1$, we find $\tau_{mix} \sim 3.4\text{x}10^{-3}$s. Thus we expect "complete mixing" to occur in $\sim 68\text{x}10^{-3}$s after energy deposition by the return stroke. If, as in Fig. 1, the volume of the channel increases to ~ 20 times its original value during that time, we will have $\sim 20\text{cm}^3$ of ambient air mixed with each 1cm^3 of air initially in the channel. This gives us a mixing rate (F_0 in the notation of Hill <u>et al.</u>, 1980) of $\sim 300\text{cm}^3$/s per cm^3 of air originally in the channel, which falls in the upper end of the range considered by Hill <u>et al</u>. Because we have not treated the cumulative effects of the various asymmetry types and because some of the numbers which we have used are only rough estimates, we feel that 300cm^3/s should be treated as an order of magnitude estimate of F_0. Given our results, the estimates of Hill <u>et al</u>. (1980) for global NO_x production by lightning appear to be quite reasonable.

Acknowledgments

This paper reports the results of work which was performed at the Naval Research Laboratory by members of the Laboratory for Computational Physics and the Plasma Physics Division. The Office of Naval Research and the Defense Advanced Research Projects Agency provided the funding for this work. The authors also gratefully acknowledge the helpful comments of Dr. A. E. Robson during the preparation of this report.

References

Batchelor, G. K., 1967: An Introduction to Fluid Dynamics, New York, Cambridge University Press, 507 - 593.

Boris, J. P., 1977: Dynamic Stabilization of the Imploding Shell Rayleigh-Taylor Instability, Comments on Plasma Physics and Controlled Fusion (3), No. 1, 1-13.

Greig, J. R., D. W. Koopman, R. F. Fernsler, R. E. Pechacek, I. M. Vitkovitsky, and A. W. Ali, 1978: Electrical Discharges Guided by Pulsed CO_2 - Laser Radiation, Phys. Rev. Lett., 41, 174-177.

Hill, R. D., 1971: Channel Heating in Return-Stroke Lightning, J. Geophys. Res., 76, 637 - 645.

Hill, R. D., 1979: On the Production of Nitric Oxide by Lightning, Geophys. Res. Lett., 6, 945 - 947.

Hill, R. D., R. G. Rinker, and H. Dale Wilson, 1980: Atmospheric Nitrogen Fixation by Lightning, J. Atmos. Sci., 37, 179 - 192.

Footnotes

1. JAYCOR, Inc., Alexandria, Virginia

2. Boris, J. P., and J. M. Picone, 1980;"Beam Generated Vorticity and Convective Channel Mixing," NRL Memorandum Report 4327, [available through DDC and NTIS].

APPENDIX A

In this appendix, we give a heuristic proof of the relation (11) for convective cooling of discharge channels:

$$\frac{\Delta V_{cool}}{V_0} \approx \frac{\Delta t_{cool}}{\tau_{mix}} . \qquad (11)$$

We define Δt_{cool} to be the time interval during which the channel cools convectively to ambient temperature; ΔV_{cool} is the increase in channel volume due to entrainment of ambient air over the time interval Δt_{cool}; V_0 is the channel volume before appreciable mixing; and τ_{mix} has been defined as the time required for a fluid element to move from one side of the channel to the opposite side. We assume that the channel is cylindrical with radius R_1 and length Z and that a vortex filament pair exists at $\bar{x} = 0$, $\bar{y} \sim \pm R_1$.

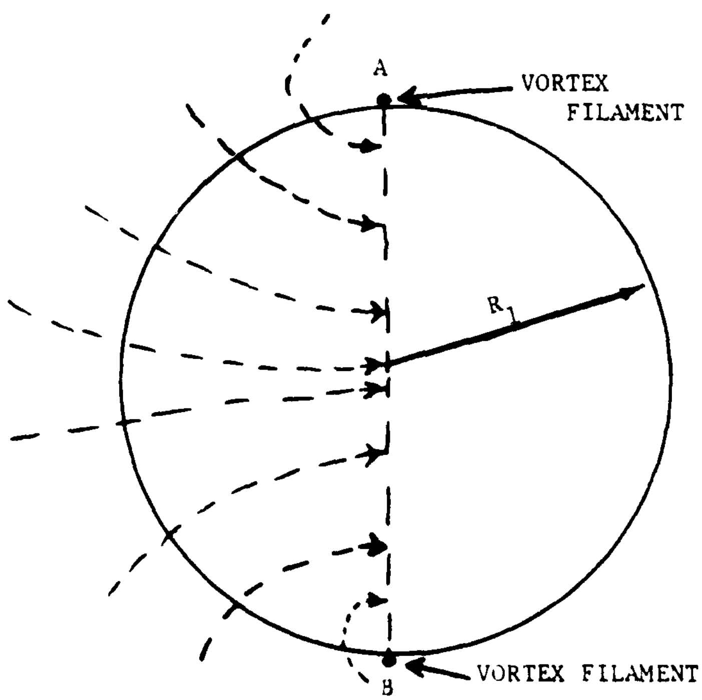

Fluid elements on different streamlines move at different speeds, and thus adjacent fluid elements on different streamlines will soon have different temperatures and densities. Thermal conduction and molecular diffusion will occur rapidly between adjacent fluid elements since their displacement is small, and we therefore have enhanced cooling over the same situation (hot channel in cool ambient air) without convection. In addition, the experimental data (see Fig. 1) indicate that turbulent mixing occurs as the surrounding air is pulled into the hot channel. These factors should combine to produce rapid, efficient mixing, and the continued entrainment of ambient air will cause the channel to expand. To obtain the volume increase over the interval Δt_{cool}, we may therefore compute the volume of ambient air flowing into the channel per unit time. This is given by (Batchelor, pp. 75-76)

$$\frac{dV}{dt} = \int_{\substack{\text{SURFACE} \\ \overline{ABZ}}} \underline{v} \cdot \underline{da} \tag{1A}$$

where $\underline{v}$ is the fluid velocity and the integral is taken over the surface defined by the channel axis Z and the dashed line $\overline{AB}$ in the figure. Given the definition of τ_{mix}, we may approximate v by:

$$v \sim \frac{2R_1}{\tau_{mix}} . \tag{2A}$$

The area of the surface $\overline{ABZ}$ is

$$a = 2R_1 Z. \tag{3A}$$

Thus the volume of ambient air flowing into the channel per unit time is

$$\frac{dV}{dt} \sim \frac{2R_1}{\tau_{mix}} \times 2R_1 Z = \frac{4R_1^{\,2} Z}{\tau_{mix}} \quad . \tag{4A}$$

We now estimate the volume increase of the channel (ΔV_{cool}) during the cooling time interval (Δt_{cool}) by integrating (4A) over Δt_{cool}. This gives us

$$\Delta V_{cool} \sim \frac{dV}{dt} \; \Delta t_{cool} \sim \frac{4R_1^{\,2} Z}{\tau_{mix}} \Delta t_{cool} \tag{5A}$$

The original channel volume is given by

$$V_0 = \pi R_1^{\,2} Z \tag{6A}$$

so that

$$\frac{\Delta V_{cool}}{V_0} \sim \frac{4}{\pi} \frac{\Delta t_{cool}}{\tau_{mix}} \sim \frac{\Delta t_{cool}}{\tau_{mix}} \tag{7A}$$

This relation is independent of initial channel size, and the volume increase will be primarily determined by the channel temperature T_1 just before mixing begins and the ambient temperature T_ω. For both lightning and the laboratory discharges $T_1 \sim 3000\text{–}5000$ K and $T_\omega \sim 300$ K. Thus $\frac{\Delta V_{cool}}{V_0}$ and $\frac{\Delta t_{cool}}{\tau_{mix}}$ are about the same in the two cases. So our use of $\Delta t_{cool} \sim 20\ \tau_{mix}$ for lightning appears to be justified.

We note that (1A) can be restated as

$$\frac{\Delta V_{cool}}{\Delta t_{cool}} = \frac{V_0}{\tau_{mix}} \quad . \tag{8A}$$

The left hand side is just the average "mixing rate" for the problem. Thus the factor τ_{mix} indeed appears to be a fundamental time scale for convective channel cooling. Further investigation of the physical significance of τ_{mix} should result in a more elegant proof of (11).

DISTRIBUTION LIST

1. Commander
   Naval Sea Systems Command
   Department of the Navy
   Washington, D.C. 20363
   ATTN: NAVSEA 03H (Dr. C. F. Sharn)

2. Central Intelligence Agency
   P. O. Box 1925
   Washington, D. C. 20013
   ATTN: Dr. C. Miller/OSI

3. Air Force Weapons Laboratory
   Kirtland Air Force Base
   Albuquerque, New Mexico 87117
   ATTN: Lt. Col. J. H. Havey
   Maj. Harold Dogliani
   Dr. David Straw

4. U. S. Army Ballistics Research Laboratory
   Aberdeen Proving Ground, Maryland 21005
   ATTN: Dr. D. Eccleshall (DRXBR-BM)

5. Ballistic Missile Defense Advanced Technology Center
   P. O. Box 1500
   Huntsville, Alabama 35807
   ATTN: Dr. L. Harvard (BMDSATC-1)

6. B-K Dynamics Inc.
   15825 Shady Grove Road
   Rockville, Maryland 20850
   ATTN: Mr. I. Kuhn

7. Intelcom Rad Tech
   P. O. Box 81087
   San Diego, California 92183
   ATTN: Mr. W. Selph

8. Lawrence Livermore Laboratory
   University of California
   Livermore, California 94550
   ATTN: Dr. R. J. Briggs
   Dr. T. Fessenden
   Dr. E. P. Lee

9. Mission Research Corporation
   735 State Street
   Santa Barbara, California 93102
   ATTN: Dr. C. Longmire
   Dr. N. Carron

10. Pulse Sciences Inc.
Suite 610
1615 Broadway
Oakland, California 94612
ATTN: Dr. S. Putnam

11. Science Applications, Inc.
1200 Prospect Street
LaJolla, California 92037
ATTN: Dr. M. P. Fricke
Dr. W. A. Woolson

12. Science Applications, Inc.
Security Office
5 Palo Alto Square, Suite 200
Palo Alto, California 94304
ATTN: Dr. R. R. Johnson
Dr. Leon Feinstein
Dr. J. G. Siambis

13. Science Applications, Inc.
1651 Old Meadow Road
McLean, Virginia 22101
ATTN: Mr. W. Chadsey

14. Science Applications, Inc.
8201 Capwell Drive
Oakland, California 94621
ATTN: Dr. J. E. Reaugh

15. Naval Surface Weapons Center
White Oak Laboratory
Silver Spring, Maryland 20910
ATTN: Mr. R. J. Biegalski
Dr. R. Cawley
Dr. J. W. Forbes
Dr. D. L. Love
Dr. C. M. Huddleston
Mr. W. M. Hinckley
Dr. G. E. Hudson
Mr. G. J. Peters
Mr. N. E. Scofield
Dr. E. C. Whitman
Dr. M. H. Cha
Dr. H. S. Uhm
Dr. R. B. Fiorito

16. C. S. Draper Laboratories
Cambridge, Massachusetts 02139
ATTN: Dr. E. Olsson
Dr. L. Matson

17. M. I. T. Lincoln Laboratories
P. O. Box 73
Lexington, Massachusetts 02173
ATTN: Dr. J. Salah

18. Physical Dynamics, Inc.
P. O. Box 1883
LaJolla, California 92038
ATTN: Dr. K. Brueckner

19. Office of Naval Research
Department of the Navy
Arlington, Virginia 22217
ATTN: Dr. W. J. Condell (Code 421)

20. Avco Everett Research Laboratory
2385 Revere Beach Pkwy.
Everett, Massachusetts 02149
ATTN: Dr. R. Patrick
Dr. Dennis Reilly

21. Defense Technical Information Center
Cameron Station
5010 Duke Street
Alexandria, Virginia 22314 (12 copies)

22. Naval Research Laboratory
Washington, D. C. 20375
ATTN: M. Lampe - Code 4792
M. Friedman - Code 4700.1
J. R. Greig - Code 4763 (50 copies)
I. M. Vitkovitsky - Code 4770
T. Coffey - Code 4000
Superintendent, Plasma Physics Div. - Code 4700 (25 copies)
Library - Code 2628 (20 copies)
A. Ali - Code 4700.1T
D. Book - Code 4040
J. Boris - Code 4040
S. Kainer - Code 4790
A. Robson - Code 4760
M. Picone - Code 4040
D. Spicer - Code 4169
M. Raleigh - Code 4763
R. Pechacek - Code 4763
J. D. Sethian - Code 4762
K. A. Gerber - Code 4762
D. N. Spector - Code 4762

23. Defense Advanced Research Projects Agency
1400 Wilson Blvd.
Arlington, Virginia 22209
ATTN: Dr. J. Mangano
Dr. J. Bayless

24. JAYCOR
205 S. Whiting St.
Alexandria, Virginia 22304
ATTN: Drs. D. Tidman
R. Hubbard
J. Gillory

25. JAYCOR
Naval Research Laboratory
Washington, D. C. 20375
ATTN: Dr. R. Fernsler - Code 4770
Dr. G. Joyce - Code 4790
Dr. S. Goldstein - Code 4770

26. SAI
Naval Research Laboratory
Washington, D. C. 20375
ATTN: A. Drobot - Code 4790
W. Sharp - Code 4790

27. Physics International, Inc.
2700 Merced Street
San Leandro, California 94577
ATTN: Dr. J. Maenchen
Dr. E. Goldman

28. Mission Research Corp
1400 San Mateo, S.E., Suite A
Albuquerque, New Mexico 87108
ATTN: Dr. Brendan Godfrey
Dr. Carl Ekdahl

29. Princeton University
Plasma Physics Laboratory
Princeton, New Jersey 08540
ATTN: Dr. F. Perkins, Jr.

30. McDonnell Douglas Research Laboratories
Dept. 223, Bldg. 33, Level 45
Box 516
St. Louis, Missouri 63166
ATTN: Dr. Michael Greenspan
Dr. J. C. Leader

31. Cornell University
Ithaca, New York 14853
ATTN: Prof. David Hammer

32. Sandia Laboratories
Albuquerque, New Mexico 87185
ATTN: Dr. Bruce Miller
Dr. Barbara Epstein
Dr. John Olsen
Dr. Don Cook

33. University of California
Physics Department
Irvine, California 92717
ATTN: Dr. Gregory Benford

34. Naval Air Systems Command
Washington, D. C. 20361
ATTN: Dr. R. J. Wasneski, Code AIR-350F

35. Beers Associates, Inc.
P. O. Box 2549
Reston, Virginia 22090
ATTN: Dr. Douglas Strickland

36. U. S. Department of Energy
Washington, D. C. 20545
Office of Fusion Energy, ATTN: Dr. W. F. Dove
Office of Inertial Fusion, ATTN: Dr. T. Godlove

37. AFOSR/NP
Bolling Air Force Base
Washington, D. C. 20331
ATTN: Capt. R. L. Gullickson